(Preprint) AAS 17-124

KINEMATIC STEERING LAW ENABLING CONICALLY CONSTRAINED SPACECRAFT ATTITUDE CONTROL

Manuel Diaz Ramos* **and Hanspeter Schaub†**

This paper presents a novel algorithm for attitude control of a spacecraft with reaction wheels subjected to inclusion and exclusion conic constraints using a rate-based attitude servo system. The tracking errors are defined using Modified Rodrigues Parameters (MRPs) to yield a non-singular description. Lyapunov theory and logarithmic barrier potential functions are used to derive a kinematic steering law suitable for both attitude regulation and tracking scenarios. Conditions for switching between constrained and unconstrained laws are discussed to not have the avoidance considerations impact rotational motion that does not approach avoided orientations. A tracking problem with inclusion and exclusion attitude zones is simulated.

INTRODUCTION

Unconstrained autonomous attitude control has been extensively addressed in literature. However, spacecraft reorientation may have several restrictions. In fact, certain orientations might not be desired while maneuvering. An example is a spacecraft carrying sensitive optical payloads, such as telescopes or cameras, that cannot be exposed to direct sunlight. Bright celestial objects may thus impose constraints to a maneuver. On the other hand, a change in attitude could be performed while keeping certain instruments, e.g. antennas, pointing into a definite region in space. Ultimately, attitude constraints can be viewed as either exclusion or inclusion zones, usually defined by cones in space around either a forbidden or a mandatory nominal direction.

The existing techniques for studying the constrained attitude control problem may be classified into six different groups.[1] A geometric approach uses geometric relations to pre-compute trajectories that avoid the constraint manifolds.[2,3] These techniques are relatively simple but do not scale well when the number of constraints grow.[1] Constraint Monitor Algorithms (CMT) use a predictor-corrector approach to change the trajectory in real time when approaching a constraint.[1] This method has been successfully tested in real missions, such as Cassini[4,5] and Deep-Space-1.[1] Randomized algorithms use graphs and random search to go from an initial to a final attitude avoiding all constraints.[6] The approach has mainly two drawbacks: convergence can be guaranteed only in a probabilistic sense and computational time grows dramatically with the size of the graph. The set of techniques known as Semi-Definite Programming (SDP) algorithms and Quadratically Constrained Quadratic Programming (QCQP) utilize optimization tools for computing an optimal control solution while avoiding all constraints.[1,7,8] A recently developed new framework divides the attitude space into discrete cells and uses searching algorithms like A^* to find an optimal solution to the constrained problem.[9,10] Finally, potential function-based algorithms use Lyapunov theory to design control laws that converge to the target while evading constraints. This approach has already been tested with euler angles[11] and quaternions.[12,13] However, these algorithms only solve the regulation problem.

Modified Rodrigues Parameters (MRPs) constitute a non-unique minimal-set attitude representation. This fact can be used to switch the parameters at the unit sphere in order to avoid their only singularity while

*Graduate Student, Aerospace Engineering Sciences, University of Colorado Boulder.
†Alfred T. and Betty E. Look Professor of Engineering, Department of Aerospace Engineering Sciences, University of Colorado, 431 UCB, Colorado Center for Astrodynamics Research, Boulder, CO 80309-0431.

naturally overcoming the unwinding[14] phenomenon, making a control scheme to always follow the shortest path.[15]

Kinematic steering laws permit dividing the attitude and angular velocity control strategies into two completely separate loops, simplifying the synthesis of control laws. Using this scheme, an angular velocity loop, usually known as servo, is controlled by a kinematic loop.

In this work, a kinematic steering law using MRPs that permits autonomous attitude control and static constraint enforcement at the same time is proposed. Constraint geometry is discussed and Lyapunov direct method is used in order to synthesize the kinematic steering law. Reaction Wheels (RW) are used as attitude actuators. The problem of wheel torque saturation is addressed.

The paper is organized as follows. After a brief introduction of the kinematics (MRPs), dynamics (rigid body spacecraft with RW), and the unconstrained steering law used, conic static constraints are presented showing a novel description as a function of MRPs. The tracking problem with conic constraints is then developed with heuristic algorithms for asymptotic stability and switching between the constrained and unconstrained steering laws. Finally, numerical results are shown.

PRELIMINARIES

Modified Rodrigues Parameters

The MRPs are a minimal parametrization set of the rotation group SO(3). The MRP vector $\boldsymbol{\sigma}$ is defined in terms of the quaternion $\boldsymbol{\beta} = \begin{bmatrix}\beta_0 & \beta_1 & \beta_2 & \beta_3\end{bmatrix}^T$ or the principal rotation vector representation $(\hat{\boldsymbol{e}}, \Phi)$ as[15]

$$\boldsymbol{\sigma} = \frac{1}{1+\beta_0}\begin{bmatrix}\beta_1 & \beta_2 & \beta_3\end{bmatrix}^T = \tan\left(\frac{\Phi}{4}\right)\hat{\boldsymbol{e}} \tag{1}$$

where β_0 represents the scalar part of the quaternion. The representation is singular whenever $\beta_0 = -1$, where the rotation angle $\Phi = \pm 360^\circ$.

The quaternion representation is not unique. In fact, since $\boldsymbol{\beta}$ and $-\boldsymbol{\beta}$ represent the same attitude, $\boldsymbol{\sigma}$ and $\boldsymbol{\sigma}^s$, known as the shadow set, also represent the same orientation, where[15]

$$\boldsymbol{\sigma}^s = -\frac{1}{1-\beta_0}\begin{bmatrix}\beta_1 & \beta_2 & \beta_3\end{bmatrix}^T = -\frac{\boldsymbol{\sigma}}{\boldsymbol{\sigma}^T\boldsymbol{\sigma}} \tag{2}$$

Equation (1) shows that short rotations ($\Phi \leq 180^\circ$) have $|\boldsymbol{\sigma}| \leq 1$. Using this fact and the shadow set, the general approach is to switch between MRP representations in the unit sphere in order to avoid the singularity while always describing short rotations.[15]

The rotation matrix $[C(\boldsymbol{\sigma})]$, also represented as $[PQ]$ when describes the orientation of a frame $\mathcal{P}$ relative to a frame $\mathcal{Q}$, can be computed from the MRP $\boldsymbol{\sigma}$ (or $\boldsymbol{\sigma}_{\mathcal{P}/\mathcal{Q}}$) as[15]

$$[C(\boldsymbol{\sigma})] = [I_{3\times 3}] + \frac{8[\tilde{\boldsymbol{\sigma}}]^2 - 4(1-\boldsymbol{\sigma}^T\boldsymbol{\sigma})[\tilde{\boldsymbol{\sigma}}]}{(1+\boldsymbol{\sigma}^T\boldsymbol{\sigma})^2} \tag{3}$$

where $[\tilde{\boldsymbol{\sigma}}]$ is the associated skew-symmetric matrix.[15]

To transform the Direction Cosine Matrix (DCM) into MRPs, Shepard's method can be used to compute quaternions from DCM[16] and then Equation (1) can be utilized to calculate the MRPs.

The MRP kinematic differential equation is given by[15]

$$\dot{\boldsymbol{\sigma}} = \frac{1}{4}\left[(1-\boldsymbol{\sigma}^T\boldsymbol{\sigma})[I_{3\times 3}] + 2[\tilde{\boldsymbol{\sigma}}] + \boldsymbol{\sigma}\boldsymbol{\sigma}^T\right]\boldsymbol{\omega} = \frac{1}{4}[B(\boldsymbol{\sigma})]\boldsymbol{\omega} \tag{4}$$

If $\boldsymbol{\sigma}$ represents the attitude of frame $\mathcal{P}$ relative to $\mathcal{Q}$ (noted as $\boldsymbol{\sigma}_{\mathcal{P}/\mathcal{Q}}$), then $\boldsymbol{\omega}$ is the angular velocity of frame $\mathcal{P}$ relative to $\mathcal{Q}$ written in $\mathcal{P}$-frame components (also noted as ${}^{\mathcal{P}}\boldsymbol{\omega}_{\mathcal{P}/\mathcal{Q}}$).

Rigid-Body Dynamics with Reaction Wheels

The rotational equations of motion of a rigid spacecraft with N_{RW} perfectly symmetric and balanced Reaction Wheels (RW) are given by[15]

$$[I_{\text{RW}}]\dot{\boldsymbol{\omega}} = -[\tilde{\boldsymbol{\omega}}]\left([I_{\text{RW}}]\boldsymbol{\omega} + [G_{\text{s}}]\boldsymbol{h}_{\text{s}}\right) - [G_{\text{s}}]\boldsymbol{u}_{\text{s}} + \boldsymbol{L} \tag{5}$$

where

$$[I_{\text{RW}}] = [I_{\text{s}}] + \sum_{i=1}^{N_{\text{RW}}} (J_{t_i}\hat{\boldsymbol{g}}_{\boldsymbol{t_i}}\hat{\boldsymbol{g}}_{\boldsymbol{t_i}}{}^T + J_{g_i}\hat{\boldsymbol{g}}_{\boldsymbol{g_i}}\hat{\boldsymbol{g}}_{\boldsymbol{g_i}}{}^T) \tag{6}$$

$$[G_{\text{s}}] = \begin{bmatrix}\hat{\boldsymbol{g}}_{\boldsymbol{s_1}} & \cdots & \hat{\boldsymbol{g}}_{\boldsymbol{s_i}} & \cdots & \hat{\boldsymbol{g}}_{\boldsymbol{s}_{N_{\text{RW}}}}\end{bmatrix} \tag{7}$$

$$\boldsymbol{h}_{\text{s}} = \begin{bmatrix}J_{s_1}(\hat{\boldsymbol{g}}_{\boldsymbol{s_1}}{}^T\,\boldsymbol{\omega} + \Omega_1) & \cdots & J_{s_i}(\hat{\boldsymbol{g}}_{\boldsymbol{s_i}}{}^T\,\boldsymbol{\omega} + \Omega_i) & \cdots & J_{s_N}(\hat{\boldsymbol{g}}_{\boldsymbol{s}_{N_{\text{RW}}}}{}^T\,\boldsymbol{\omega} + \Omega_{N_{\text{RW}}})\end{bmatrix}^T \tag{8}$$

$[I_{\text{s}}]$ is the inertia tensor of the system with the wheels considered as point masses. A principal-axis frame $\mathcal{W}_i : \{\hat{\boldsymbol{g}}_{\boldsymbol{s_i}}, \hat{\boldsymbol{g}}_{\boldsymbol{t_i}}, \hat{\boldsymbol{g}}_{\boldsymbol{g_i}}\}$ is attached to each RW, where $\hat{\boldsymbol{g}}_{\boldsymbol{s_i}}$ is the direction of the spin axis. $[I_{w_i}] = \text{diag}(\begin{bmatrix}J_{s_i} & J_{t_i} & J_{g_i}\end{bmatrix})$ is the inertia matrix of each wheel written in the $\mathcal{W}$ frame relative to its center of mass. Ω_i is the angular velocity of the RW i relative to the spacecraft. The vector $\boldsymbol{u}_{\text{s}}$ contains the torques applied to each RW axis. $\boldsymbol{L}$ is the resultant external torque applied to the spacecraft.

The vector $\boldsymbol{\omega}$ is a shorthand notation for $\boldsymbol{\omega}_{\mathcal{B}/\mathcal{N}}$, where $\mathcal{B}$ is a body-fixed frame and $\mathcal{N}$ is an inertial frame. The over-dot symbol ($\dot{\bullet}$) represents an inertial derivative while the prime symbol ($\bullet'$) represents a derivative with respect to the body frame. Although the equations of motion can be solved in any frame, it will be assumed that every vector and tensor are written in the body-fixed frame $\mathcal{B}$.

In this paper, the RW torque may saturate. In other words, there is a maximum torque $u_{s_{\max}}$ that is applied to each reaction wheel.

Unconstrained Problem Using a Steering Law

The unconstrained attitude problem can be solved using the Lyapunov direct method with a Liapunov function combining attitude and angular velocity.[15] However, two separate feedback loops may also be setup,[17] in a rather similar way as the Backstepping Control method.[18,19] A faster loop controls angular velocity. An outer, slower loop, or steering law, controls attitude, taking angular velocity as a control force. Using two different loops for attitude and angular velocity has some advantages. First, the kinematic model given by Equation (4) is exact. Second, the synthesis of control laws is simplified. Third, as this paper demonstrates, the angular velocity loop does not need to be changed when static constraints are added. The following notation assumes that every angular velocity vector is written in the body frame.

The goal of the control scheme is to steer the body frame $\mathcal{B}$ to the reference frame $\mathcal{R}$. In other words, the relative attitude $\boldsymbol{\sigma}_{\mathcal{B}/\mathcal{R}}$ and angular velocity $\boldsymbol{\omega}_{\mathcal{B}/\mathcal{R}}$ are to be driven to zero. If the given attitude $\boldsymbol{\sigma}_{\mathcal{R}/\mathcal{N}}$ is not constant, the problem is usually known as the tracking control problem.

Consider the following Lyapunov candidate function[15]

$$V(\boldsymbol{\sigma}_{\mathcal{B}/\mathcal{R}}) = 2\ln\left(1 + \boldsymbol{\sigma}_{\mathcal{B}/\mathcal{R}}^T\boldsymbol{\sigma}_{\mathcal{B}/\mathcal{R}}\right) \tag{9}$$

Using Equation (4) it can be immediately shown that

$$\dot{V}(\boldsymbol{\sigma}_{\mathcal{B}/\mathcal{R}}) = \boldsymbol{\sigma}_{\mathcal{B}/\mathcal{R}}^T\boldsymbol{\omega}_{\mathcal{B}/\mathcal{R}} \tag{10}$$

Let $\mathcal{B}^*$ be the desired body orientation and $\boldsymbol{\omega}_{\mathcal{B}^*/\mathcal{R}}$ the desired angular velocity vector. Making

$$\boldsymbol{\omega}_{\mathcal{B}^*/\mathcal{R}} = -\boldsymbol{f}(\boldsymbol{\sigma}_{\mathcal{B}/\mathcal{R}}) \tag{11}$$

where $\boldsymbol{f}(\boldsymbol{\sigma}_{\mathcal{B}/\mathcal{R}})$ is an even function such that

$$\boldsymbol{\sigma}_{\mathcal{B}/\mathcal{R}}^T \boldsymbol{f}(\boldsymbol{\sigma}_{\mathcal{B}/\mathcal{R}}) > 0 \tag{12}$$

The Lyapunov rate will, thus, be negative definite

$$\dot{V}(\boldsymbol{\sigma}_{\mathcal{B}/\mathcal{R}}) = -\boldsymbol{\sigma}_{\mathcal{B}/\mathcal{R}}^T \boldsymbol{f}(\boldsymbol{\sigma}_{\mathcal{B}/\mathcal{R}}) < 0 \qquad \forall \boldsymbol{\sigma}_{\mathcal{B}/\mathcal{R}} \neq \mathbf{0} \tag{13}$$

In this paper, the smoothly saturated function given by

$$f_i(x_i) = \frac{2\omega_{\max}}{\pi} \arctan\left(\frac{\pi}{2\omega_{\max}}(K_1 x_i + K_3 x_i^3)\right) \quad i = 1,2,3 \tag{14}$$

is used. $\boldsymbol{f}(\boldsymbol{\sigma}_{\mathcal{B}/\mathcal{R}}) = \begin{bmatrix} f_1(\sigma_1) & f_2(\sigma_2) & f_3(\sigma_3) \end{bmatrix}^T$.

A servo sub-system is utilized to produce the required torques to make the body rates track the desired body rates commanded by the steering law. The tracking error is defined as

$$\boldsymbol{\omega}_{\mathcal{B}/\mathcal{B}^*} = \boldsymbol{\omega}_{\mathcal{B}/\mathcal{N}} - \boldsymbol{\omega}_{\mathcal{B}^*/\mathcal{N}} \tag{15}$$

where $\boldsymbol{\omega}_{\mathcal{B}^*/\mathcal{N}} = \boldsymbol{\omega}_{\mathcal{B}^*/\mathcal{R}} + \boldsymbol{\omega}_{\mathcal{R}/\mathcal{N}}$, $\boldsymbol{\omega}_{\mathcal{B}^*/\mathcal{R}}$ is the kinematic steering rate command and $\boldsymbol{\omega}_{\mathcal{R}/\mathcal{N}}$ is an input coming from the attitude navigation solution. To create a rate-servo that is robust to unmodeled torques,[15] the integral term $\boldsymbol{z}$ is defined as

$$\boldsymbol{z} = \int_{t_0}^{t} \boldsymbol{\omega}_{\mathcal{B}/\mathcal{B}^*} \, \mathrm{d}d\tau \tag{16}$$

Consider the Lyapunov candidate function[17]

$$V_{\boldsymbol{\omega}}(\boldsymbol{\omega}_{\mathcal{B}/\mathcal{B}^*}, \boldsymbol{z}) = \frac{1}{2}\boldsymbol{\omega}_{\mathcal{B}/\mathcal{B}^*}^T [I_{\mathrm{RW}}] \boldsymbol{\omega}_{\mathcal{B}/\mathcal{B}^*} + \frac{1}{2}\boldsymbol{z}^T [K_{\mathrm{I}}] \boldsymbol{z} \tag{17}$$

where $[K_{\mathrm{I}}]$ is a positive definite matrix.

Thus

$$\dot{V}_{\boldsymbol{\omega}}(\boldsymbol{\omega}_{\mathcal{B}/\mathcal{B}^*}, \boldsymbol{z}) = \boldsymbol{\omega}_{\mathcal{B}/\mathcal{B}^*}^T \left([I_{\mathrm{RW}}] \boldsymbol{\omega}'_{\mathcal{B}/\mathcal{B}^*} + [K_{\mathrm{I}}] \boldsymbol{z} \right) \tag{18}$$

Using the identities $\boldsymbol{\omega}'_{\mathcal{B}/\mathcal{N}} = \dot{\boldsymbol{\omega}}_{\mathcal{B}/\mathcal{N}}$ and $\boldsymbol{\omega}'_{\mathcal{R}/\mathcal{N}} = \dot{\boldsymbol{\omega}}_{\mathcal{R}/\mathcal{N}} - \boldsymbol{\omega}_{\mathcal{B}/\mathcal{N}} \times \boldsymbol{\omega}_{\mathcal{R}/\mathcal{N}}$, and Equation (5)

$$\begin{aligned} \dot{V}_{\boldsymbol{\omega}}(\boldsymbol{\omega}_{\mathcal{B}/\mathcal{B}^*}, \boldsymbol{z}) = \boldsymbol{\omega}_{\mathcal{B}/\mathcal{B}^*}^T \big[& -[\tilde{\boldsymbol{\omega}}_{\mathcal{B}/\mathcal{N}}] \left([I_{\mathrm{RW}}] \boldsymbol{\omega}_{\mathcal{B}/\mathcal{N}} + [G_{\mathrm{s}}] \boldsymbol{h}_{\mathrm{s}} \right) - [G_{\mathrm{s}}] \boldsymbol{u}_{\mathrm{s}} + \boldsymbol{L} + [K_{\mathrm{I}}] \boldsymbol{z} \\ & - [I_{\mathrm{RW}}] (\boldsymbol{\omega}'_{\mathcal{B}^*/\mathcal{R}} + \dot{\boldsymbol{\omega}}_{\mathcal{R}/\mathcal{N}} - \boldsymbol{\omega}_{\mathcal{B}/\mathcal{N}} \times \boldsymbol{\omega}_{\mathcal{R}/\mathcal{N}}) \big] \end{aligned} \tag{19}$$

Forcing $\dot{V}_{\boldsymbol{\omega}} = -\boldsymbol{\omega}_{\mathcal{B}/\mathcal{B}^*}^T [P] \boldsymbol{\omega}_{\mathcal{B}/\mathcal{B}^*}$, with $[P]$ being a positive definite matrix, it is possible to write

$$[G_{\mathrm{s}}] \boldsymbol{u}_{\mathrm{s}} = \boldsymbol{L_r} \tag{20}$$

where

$$\boldsymbol{L_r} = [P] \boldsymbol{\omega}_{\mathcal{B}/\mathcal{B}^*} + [K_{\mathrm{I}}] \boldsymbol{z} - [\tilde{\boldsymbol{\omega}}_{\mathcal{B}/\mathcal{N}}] \left([I_{\mathrm{RW}}] \boldsymbol{\omega}_{\mathcal{B}/\mathcal{N}} + [G_{\mathrm{s}}] \boldsymbol{h}_{\mathrm{s}} \right) - [I_{\mathrm{RW}}] (\boldsymbol{\omega}'_{\mathcal{B}^*/\mathcal{R}} + \dot{\boldsymbol{\omega}}_{\mathcal{R}/\mathcal{N}} - \boldsymbol{\omega}_{\mathcal{B}/\mathcal{N}} \times \boldsymbol{\omega}_{\mathcal{R}/\mathcal{N}}) \tag{21}$$

The RW torques can be computed in several different ways. In this paper, the minimum norm inverse is used[15]

$$\boldsymbol{u}_{\mathrm{s}} = [G_{\mathrm{s}}]^T ([G_{\mathrm{s}}][G_{\mathrm{s}}]^T)^{-1} \boldsymbol{L_r} \tag{22}$$

The body frame derivative $\boldsymbol{\omega}'_{\mathcal{B}^*/\mathcal{R}}$ is calculated numerically.

Equations (11) and (22) can be used to control a spacecraft's attitude using reaction wheels without constraints. The servo sub-system needs to have a faster frequency response.

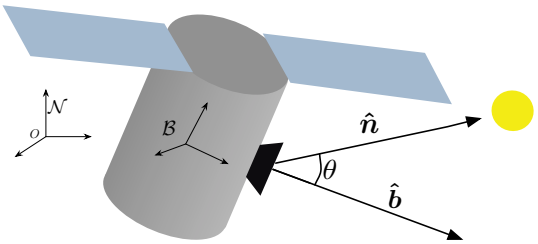

Figure 1. Static constraint geometry.

CONSTRAINT GEOMETRY

Constraints can be classified into several groups.[1] In this work, only constraints that depend on the current attitude are considered. Henceforth, those constraints will be called static constraints because they only depend on the current orientation, and not on the angular velocity.

The conic constraint is a particular static constraint illustrated in Figure 1 where an inertial unit vector $\hat{\boldsymbol{n}}$ defines an exclusion or inclusion cone around it. Meshabi et. al.[1] call these constraints Type-I constraints. The goal is to slew a spacecraft avoiding a unit vector $\hat{\boldsymbol{b}}$ entering the cone. The security angle is given by θ_{min}, while θ is the instantaneous angle between both vectors. In a typical application $\hat{\boldsymbol{n}}$ can be a unit vector pointing towards the sun (approximately inertially fixed) while $\hat{\boldsymbol{b}}$ is the boresight vector of a camera (body fixed). Mathematically, the condition can be easily described as[5]

$$\hat{\boldsymbol{n}} \cdot \hat{\boldsymbol{b}} = \cos(\theta) < \cos(\theta_{\text{min}}) \tag{23}$$

Conic constraints where $\hat{\boldsymbol{n}}$ is inertially fixed and $\hat{\boldsymbol{b}}$ is body-fixed can thus be written introducing the rotation matrix $[BN]$ as

$$C_{[BN]}([BN]) = \cos(\theta) - \cos(\theta_{\text{min}}) = \hat{\boldsymbol{n}} \cdot \hat{\boldsymbol{b}} - \cos(\theta_{\text{min}}) = {}^{\mathcal{N}}\hat{\boldsymbol{n}}^{T}[BN]^{T\,\mathcal{B}}\hat{\boldsymbol{b}} - \cos(\theta_{\text{min}}) < 0 \tag{24}$$

where the notation $C_{[BN]}$ indicates that the constraint is written as a function of the DCM.

Similarly, it might be desirable to maneuver while keeping a certain boresight vector $\hat{\boldsymbol{b}}$ inside a cone defined by $\hat{\boldsymbol{n}}$ and θ_{min}. In a typical application, the maneuver has to keep an antenna's main lobe inside a cone defined by a ground station. The mathematical condition is

$$\hat{\boldsymbol{n}} \cdot \hat{\boldsymbol{b}} = \cos(\theta) > \cos(\theta_{\text{min}}) \tag{25}$$

Considering, again, conic constraints where $\hat{\boldsymbol{n}}$ is inertially fixed and $\hat{\boldsymbol{b}}$ is body-fixed

$$C_{[BN]}([BN]) = \cos(\theta) - \cos(\theta_{\text{min}}) = \hat{\boldsymbol{n}} \cdot \hat{\boldsymbol{b}} - \cos(\theta_{\text{min}}) = {}^{\mathcal{N}}\hat{\boldsymbol{n}}^{T}[BN]^{T\,\mathcal{B}}\hat{\boldsymbol{b}} - \cos(\theta_{\text{min}}) > 0 \tag{26}$$

It is important to notice that exclusion and inclusion zones can be defined using the same constraint formulation; namely, through a function $C_{[BN]}([BN])$. It is immediately apparent from the definition that

$$-2 \leq C_{[BN]}([BN]) \leq 2 \tag{27}$$

Only constraints where $\hat{\boldsymbol{n}}$ is inertially fixed are considered, even though some of the results of the paper may be extended to consider the more general case where $\hat{\boldsymbol{n}}$ is not inertially fixed.

An expression for $\dot{C}_{[BN]}([BN])$ can be readily computed using the transport theorem[15] and the circular shift property of the triple product. If the derivatives are taken in the inertial frame under the hypothesis that $\hat{\boldsymbol{n}}$ is inertially constant and $\hat{\boldsymbol{b}}$ is body-fixed, then

$$\dot{C}_{[BN]}([BN]) = {}^{\mathcal{N}}\frac{\mathrm{d}\hat{\boldsymbol{n}}}{\mathrm{d}t} \cdot \hat{\boldsymbol{b}} + \hat{\boldsymbol{n}} \cdot {}^{\mathcal{N}}\frac{\mathrm{d}\hat{\boldsymbol{b}}}{\mathrm{d}t} = \hat{\boldsymbol{n}} \cdot (\boldsymbol{\omega}_{\mathcal{B}/\mathcal{N}} \times \hat{\boldsymbol{b}}) = (\hat{\boldsymbol{b}} \times \hat{\boldsymbol{n}}) \cdot \boldsymbol{\omega}_{\mathcal{B}/\mathcal{N}} = ([{}^{\mathcal{B}}\tilde{\boldsymbol{b}}][BN]^{\mathcal{N}}\hat{\boldsymbol{n}})^{T\,\mathcal{B}}\boldsymbol{\omega}_{\mathcal{B}/\mathcal{N}} \tag{28}$$

From Equation (3), it is possible to write

$$C_{[BN]}([BN](\boldsymbol{\sigma}_{\mathcal{B}/\mathcal{N}})) = C_{\boldsymbol{\sigma}}(\boldsymbol{\sigma}_{\mathcal{B}/\mathcal{N}}) = {}^{\mathcal{N}}\hat{\boldsymbol{n}}^{T}[BN(\boldsymbol{\sigma}_{\mathcal{B}/\mathcal{N}})]^{T\,\mathcal{B}}\hat{\boldsymbol{b}} - \cos(\theta_{\min}) \tag{29}$$

$$\dot{C}_{[BN]}([BN](\boldsymbol{\sigma}_{\mathcal{B}/\mathcal{N}})) = \dot{C}_{\boldsymbol{\sigma}}(\boldsymbol{\sigma}_{\mathcal{B}/\mathcal{N}}) = ([^{\mathcal{B}}\tilde{\boldsymbol{b}}][BN(\boldsymbol{\sigma}_{\mathcal{B}/\mathcal{N}})]^{\mathcal{N}}\hat{\boldsymbol{n}})^{T\,\mathcal{B}}\boldsymbol{\omega}_{\mathcal{B}/\mathcal{N}} \tag{30}$$

It is also possible to compute the time derivative using the gradient and the kinematic differential equation (4)

$$\dot{C}_{[BN]}([BN]) = \dot{C}_{\boldsymbol{\sigma}}(\boldsymbol{\sigma}_{\mathcal{B}/\mathcal{N}}) = \nabla C_{\boldsymbol{\sigma}}^{T}(\boldsymbol{\sigma}_{\mathcal{B}/\mathcal{N}})\dot{\boldsymbol{\sigma}}_{\mathcal{B}/\mathcal{N}} = \frac{1}{4}\nabla C_{\boldsymbol{\sigma}}^{T}(\boldsymbol{\sigma}_{\mathcal{B}/\mathcal{N}})[B(\boldsymbol{\sigma}_{\mathcal{B}/\mathcal{N}})]^{\mathcal{B}}\boldsymbol{\omega}_{\mathcal{B}/\mathcal{N}} \tag{31}$$

PROBLEM STATEMENT

Let there be N_{E} exclusion zones defined by continuous functions $C_i^E : \mathrm{SO}(3) \to \mathbb{R}$ and N_I inclusion zones defined by continous functions $C_j^I : \mathrm{SO}(3) \to \mathbb{R}$, which can be the $C_{[BN]}$ or the $C_{\boldsymbol{\sigma}}$ described in the previous section. Let $\mathcal{D}$ be such that

$$\mathcal{D} = \{x \in \mathrm{SO}(3)/C_i^E(x) < 0 \wedge C_j^I(x) > 0\} \tag{32}$$

The goal is to drive $\boldsymbol{\sigma}_{\mathcal{B}/\mathcal{R}}$ and $\boldsymbol{\omega}_{\mathcal{B}/\mathcal{R}}$ to zero while moving inside $\mathcal{D}$. The first necessary condition is that $[BN] \in \mathcal{D}$ for all possible time.

Barrier functions have been used to design control laws avoiding constraints.[11,12,20] In this paper, logarithm barrier functions[12,13,20] are used to design Lyapunov functions that converge to the reference while avoid piercing the static constraints.

CONSTRAINED CONTROL - TRACKING PROBLEM

The problem is split into two parts: a steering law and sub-servo system controlling angular velocity. The sub-servo is the same as described in the Preliminaries section for the unconstrained problem.

Consider the following Lyapunov candidate function $V : \mathcal{D} \to \mathbb{R}^{+}$

$$V(\boldsymbol{\sigma}_{\mathcal{B}/\mathcal{R}}) = 2\ln(1 + \boldsymbol{\sigma}_{\mathcal{B}/\mathcal{R}}^{T}\boldsymbol{\sigma}_{\mathcal{B}/\mathcal{R}})\left[-\frac{1}{N_E}\sum_{i=1}^{N_E}\ln\left(-\frac{C_i^E(\boldsymbol{\sigma}_{\mathcal{B}/\mathcal{N}})}{\alpha_i}\right) - \frac{1}{N_I}\sum_{j=1}^{N_I}\ln\left(\frac{C_j^I(\boldsymbol{\sigma}_{\mathcal{B}/\mathcal{N}})}{\beta_j}\right)\right] \tag{33}$$

The parameters $\alpha_i > 0$ and $\beta_j > 0$ can be chosen in several different ways with the only condition $-C_i^E(\boldsymbol{\sigma}_{\mathcal{B}/\mathcal{N}}) < \alpha_i$ and $C_j^I(\boldsymbol{\sigma}_{\mathcal{B}/\mathcal{N}}) < \beta_j \ \forall \boldsymbol{\sigma}_{\mathcal{B}/\mathcal{N}} \in \mathcal{D}$. One possibility, based on Equation (27) is to pick

$$\alpha_i = \beta_i = 2e \tag{34}$$

Therefore, the logarithm constraint terms will be between 1 and $+\infty$. Another possibility for α_i will be discussed in a next section.

Given these conditions for α_i and β_j, it is possible to show that $V(\mathbf{0}) = 0$, $V(\boldsymbol{\sigma}_{\mathcal{B}/\mathcal{R}}) > 0 \quad \forall \boldsymbol{\sigma}_{\mathcal{B}/\mathcal{N}} \in \{\mathcal{D} - \{\mathbf{0}\}\}$, and $V(\boldsymbol{\sigma}_{\mathcal{B}/\mathcal{R}}) \to +\infty$ when $C_i^E(\boldsymbol{\sigma}_{\mathcal{B}/\mathcal{N}}) \to 0$ or $C_i^I(\boldsymbol{\sigma}_{\mathcal{B}/\mathcal{N}}) \to 0$.

In order to derive a control law, the time derivative of V is computed

$$\dot{V}(\boldsymbol{\sigma}_{\mathcal{B}/\mathcal{R}}) = \frac{4\boldsymbol{\sigma}_{\mathcal{B}/\mathcal{R}}^{T}\dot{\boldsymbol{\sigma}}_{\mathcal{B}/\mathcal{R}}}{(1 + \boldsymbol{\sigma}_{\mathcal{B}/\mathcal{R}}^{T}\boldsymbol{\sigma}_{\mathcal{B}/\mathcal{R}})}\left[\frac{1}{N_E}\sum_{i=1}^{N_E} - \ln\left(-\frac{C_i^E(\boldsymbol{\sigma}_{\mathcal{B}/\mathcal{N}})}{\alpha_i}\right) - \frac{1}{N_I}\sum_{j=1}^{N_I}\ln\left(\frac{C_j^I(\boldsymbol{\sigma}_{\mathcal{B}/\mathcal{N}})}{\beta_j}\right)\right] +$$

$$2\ln(1 + \boldsymbol{\sigma}_{\mathcal{B}/\mathcal{R}}^{T}\boldsymbol{\sigma}_{\mathcal{B}/\mathcal{R}})\left[-\frac{1}{N_E}\sum_{i=1}^{N_E}\frac{\dot{C}_i^E(\boldsymbol{\sigma}_{\mathcal{B}/\mathcal{N}})}{C_i^E(\boldsymbol{\sigma}_{\mathcal{B}/\mathcal{N}})} - \frac{1}{N_I}\sum_{j=1}^{N_I}\frac{\dot{C}_j^I(\boldsymbol{\sigma}_{\mathcal{B}/\mathcal{N}})}{C_j^I(\boldsymbol{\sigma}_{\mathcal{B}/\mathcal{N}})}\right] \tag{35}$$

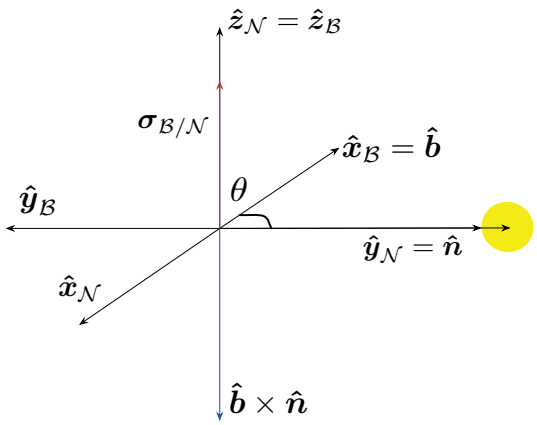

Figure 2. With perfect symmetry v_R can be 0.

Using Equations (4), (28), the fact that $\boldsymbol{\omega}_{\mathcal{B}/\mathcal{N}} = \boldsymbol{\omega}_{\mathcal{B}/\mathcal{R}} + \boldsymbol{\omega}_{\mathcal{R}/\mathcal{N}}$, and defining $\boldsymbol{v_T}$ and $\boldsymbol{u_T}$ such that

$$\boldsymbol{u_T} = 2\ln(1 + \boldsymbol{\sigma}_{\mathcal{B}/\mathcal{R}}^T \boldsymbol{\sigma}_{\mathcal{B}/\mathcal{R}}) \left[-\frac{1}{N_E} \sum_{i=1}^{N_E} \frac{([\tilde{\mathcal{B}\boldsymbol{b}}][BN]^{\mathcal{N}}\hat{\boldsymbol{n}})}{C_j^E(\boldsymbol{\sigma}_{\mathcal{B}/\mathcal{N}})} - \frac{1}{N_I} \sum_{j=1}^{N_I} \frac{([\tilde{\mathcal{B}\boldsymbol{b}}][BN]^{\mathcal{N}}\hat{\boldsymbol{n}})}{C_j^I(\boldsymbol{\sigma}_{\mathcal{B}/\mathcal{N}})} \right] \tag{36}$$

$$\boldsymbol{v_T} = \boldsymbol{\sigma}_{\mathcal{B}/\mathcal{R}} \left[\frac{1}{N_E} \sum_{i=1}^{N_E} -\ln\left(-\frac{C_i^E(\boldsymbol{\sigma}_{\mathcal{B}/\mathcal{N}})}{\alpha_i} \right) - \frac{1}{N_I} \sum_{j=1}^{N_I} \ln\left(\frac{C_j^I(\boldsymbol{\sigma}_{\mathcal{B}/\mathcal{N}})}{\beta_j} \right) \right] + \boldsymbol{u_T} \tag{37}$$

then

$$\dot{V}(\boldsymbol{\sigma}_{\mathcal{B}/\mathcal{R}}) = \boldsymbol{v_T}^{T\,\mathcal{B}}\boldsymbol{\omega}_{\mathcal{B}/\mathcal{R}} + \boldsymbol{u_T}^{T\,\mathcal{B}}\boldsymbol{\omega}_{\mathcal{R}/\mathcal{N}} \tag{38}$$

Choosing

$${}^{\mathcal{B}}\boldsymbol{\omega}_{\mathcal{B}^*/\mathcal{R}} = -\boldsymbol{f}(\boldsymbol{v_T}) - \frac{\boldsymbol{v_T}\boldsymbol{u_T}^T}{\boldsymbol{v_T}^T\boldsymbol{v_T}}{}^{\mathcal{B}}\boldsymbol{\omega}_{\mathcal{R}/\mathcal{N}} \tag{39}$$

where $\boldsymbol{f}$ is given by Equation (14)

$$\dot{V}(\boldsymbol{\sigma}_{\mathcal{B}/\mathcal{R}}) = -\boldsymbol{v_T}^T \boldsymbol{f}(\boldsymbol{v_T}) \leq 0 \tag{40}$$

It is easy to see that $\boldsymbol{v_T} = \boldsymbol{u_T} = \boldsymbol{0}$ whenever $\boldsymbol{\sigma}_{\mathcal{B}/\mathcal{R}} = \boldsymbol{0}$. However, $\ln(1 + \boldsymbol{\sigma}_{\mathcal{B}/\mathcal{R}}^T \boldsymbol{\sigma}_{\mathcal{B}/\mathcal{R}}) \to \boldsymbol{\sigma}_{\mathcal{B}/\mathcal{R}}^T \boldsymbol{\sigma}_{\mathcal{B}/\mathcal{R}}$ when $\boldsymbol{\sigma}_{\mathcal{B}/\mathcal{R}} \to 0$. Thus, even though there is a $\frac{0}{0}$ indetermination in the second term of the control law, that term tends to zero and can be ignored whenever $\boldsymbol{\sigma}_{\mathcal{B}/\mathcal{R}} \to \boldsymbol{0}$.

$\boldsymbol{v_T}$ can also be zero for other values of $\boldsymbol{\sigma}_{\mathcal{B}/\mathcal{R}}$. This situation is described in the next section.

ASYMPTOTIC STABILITY

It has been shown that the law given by (39) is almost globally Lyapunov stable but not necessarily asymptotically stable. In the special case that $\boldsymbol{v_T} = \boldsymbol{0}$ and $\boldsymbol{\sigma}_{\mathcal{B}/\mathcal{R}} \neq \boldsymbol{0}$, the law is not asymptotically stable and can even be unstable. However, it turns out that this occurs only with very specific symmetry conditions. To understand the geometric conditions that lead to this situation, consider the following regulation problem ($\boldsymbol{\sigma}_{\mathcal{R}/\mathcal{N}} = \boldsymbol{0}$), depicted in Figure 2. Let there only be one exclusion condition, given by $\hat{\boldsymbol{n}} = \hat{\boldsymbol{y}}_N$. The boresight vector is in the body $\hat{\boldsymbol{x}}$ direction: $\hat{\boldsymbol{b}} = \hat{\boldsymbol{x}}_B$. In this qualitative description, the angle θ_{min} is not relevant. The initial attitude is a rotation of $180°$ about $\hat{\boldsymbol{z}}_N$. Thus $\boldsymbol{\sigma}_{\mathcal{B}/\mathcal{N}} = \tan(180°/4)\hat{\boldsymbol{z}}_N$.

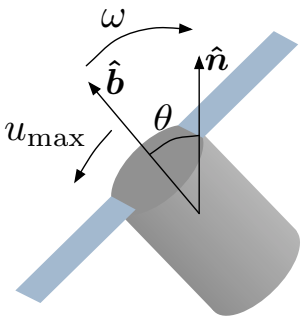

Figure 3. Worst-case scenario.

The vector $\boldsymbol{v_T}$ will be

$$\boldsymbol{v_T} = -\boldsymbol{\sigma}_{\mathcal{B}/\mathcal{N}} \ln\left(-\frac{C_1^E(\boldsymbol{\sigma}_{\mathcal{B}/\mathcal{N}})}{\alpha_1}\right) - 2\ln(1+\boldsymbol{\sigma}_{\mathcal{B}/\mathcal{N}}^T\boldsymbol{\sigma}_{\mathcal{B}/\mathcal{N}})\frac{([\tilde{\mathcal{B}}\boldsymbol{b}][BN]^{\mathcal{N}}\hat{\boldsymbol{n}})}{C_1^E(\boldsymbol{\sigma}_{\mathcal{B}/\mathcal{N}})} \tag{41}$$

A necessary (but not sufficient) condition for $\boldsymbol{v_T}$ to be zero with a non-zero $\boldsymbol{\sigma}_{\mathcal{B}/\mathcal{N}}$ is $\boldsymbol{\sigma}_{\mathcal{B}/\mathcal{N}}$ and $[\tilde{\mathcal{B}}\boldsymbol{b}][BN]^{\mathcal{N}}\hat{\boldsymbol{n}}$ to be anti-parallel. The latter is simply $\hat{\boldsymbol{b}}\times\hat{\boldsymbol{n}}$. In this particular case, that situation is possible since the attitude is a rotation about the $\hat{\boldsymbol{z}}_N$ axis and $\hat{\boldsymbol{b}}\times\hat{\boldsymbol{n}}$ is in the same direction. These saddle points can occur whenever the problem has one of such perfect symmetries. If the conic constraint is slightly tilted, the symmetry is broken, and no saddle point is reached for that attitude initial condition.

In practice, due to perturbations and numerical noise, saddle points occur very rarely. However, $\boldsymbol{v_T}$ can be arbitrarily small.

A heuristic solution to avoid these saddle points is to detect whenever $\boldsymbol{v_T}$ is small while $\boldsymbol{\sigma}_{\mathcal{B}/\mathcal{R}}$ is not and apply a very small kick to the spacecraft in any direction orthogonal to $\boldsymbol{\sigma}_{\mathcal{B}/\mathcal{R}}$ in order to break the symmetry. The heuristic algorithm is shown as Algorithm (1). $\boldsymbol{\sigma}_{\mathcal{B}/\mathcal{R}}^{\perp}$ is any orthogonal vector to $\boldsymbol{\sigma}_{\mathcal{B}/\mathcal{R}}$. γ is a small number to be chosen.

Algorithm 1 Saddle-point avoidance.

1: **if** $\|\boldsymbol{v_T}\| < 0.01$ && $\left\|\boldsymbol{\sigma}_{\mathcal{B}/\mathcal{R}}\right\| > 0.01$ **then**
2: $\quad \boldsymbol{v_T} = \gamma\boldsymbol{\sigma}_{\mathcal{B}/\mathcal{R}}^{\perp}$
3: **end if**

SWITCHING BETWEEN THE CONSTRAINED AND UNCONSTRAINED LAWS

When only exclusion constraints are defined, it might be desirable to use the unconstrained steering law given in Equation (11) when "sufficiently far" from the constraints. In order to establish what "far" means, consider the very simple worst-case planar scenario given in Figure 3. The boresight vector is going straight into a constraint cone, rotating on a plane. The inertia of the system about the fixed rotation axis is I, the angular velocity is ω and a constant available torque is given by u_{max}. The angle at time t_0 is θ_0 and the initial angular velocity is ω_0.

The problem can be stated as follows: with an inertia I, constant control torque u_{max}, and an initial velocity $\omega_0 = \omega_{\text{max}}$ given, what is the initial angle θ_0 to exactly stop the rotation at the security cone given by the angle θ_{min}? In other words, the final state should be $\theta_f = \theta_{\text{min}}$ and $\omega_f = 0$. This would mean that if $\theta > \theta_0$, the spacecraft would have enough torque capacity to avoid breaking into a conic constraint. Therefore, the unconstrained law can be used whenever $\theta > \theta_0$.

Since $\omega = -\dot{\theta}$, it is possible to write

$$\ddot{\theta} = \frac{u_{\max}}{I} \tag{42}$$

$$\dot{\theta}_f = 0 = \frac{u_{\max}}{I}(t_f - t_0) - \omega_{\max} \tag{43}$$

$$\theta_f = \theta_{\min} = \frac{1}{2}\frac{u_{\max}}{I}(t_f - t_0)^2 - \omega_{\max}(t_f - t_0) + \theta_0 \tag{44}$$

Solving for $(t_f - t_0)$ in the first equation and replacing into the second

$$\theta_0 = \frac{1}{2}\frac{I}{u_{\max}}\omega_{\max}^2 + \theta_{\min} \tag{45}$$

For a given spacecraft, I should be the maximum axis of inertia, $\omega_{\max}$ is the same maximum velocity used in the steering law in Equation (14) and $u_{\max}$ should be, at most, the maximum torque available in the poorest controllable direction. Given a maximum torque for each wheel $u_{s_{\max}}$, the minimum torque capacity for a reaction wheel array can be computed using the torque envelopes. The algorithm for computing this minimum torque capacity is given by Landis Markley et. al.[21]

$$u_{\max} \leq \min\{u_{i,j\min}; i, j = 1, ..., N_{\text{RW}}\} \tag{46}$$

$$u_{i,j\min} = u_{s_{\max}} \sum_{k=1, k\neq i,j}^{N_{\text{RW}}} |\hat{\boldsymbol{g}}_{\boldsymbol{s_k}} \cdot \hat{\boldsymbol{n}}_{\boldsymbol{ij}}| \tag{47}$$

$$\hat{\boldsymbol{n}}_{\boldsymbol{ij}} = \frac{\hat{\boldsymbol{g}}_{\boldsymbol{s_i}} \times \hat{\boldsymbol{g}}_{\boldsymbol{s_j}}}{\left\|\hat{\boldsymbol{g}}_{\boldsymbol{s_i}} \times \hat{\boldsymbol{g}}_{\boldsymbol{s_j}}\right\|} \tag{48}$$

In order to avoid chattering, two different thresholds can be defined, using a Schmitt trigger approach. The gap is defined by an angle ψ. The algorithm is shown as Algorithm 2.

Algorithm 2 Constrained-Unconstrained control switching

1: Compute $[BN]$ from $\boldsymbol{\sigma}_{\mathcal{B}/\mathcal{N}}$ using Equation (3)
2: Compute $\theta = \arccos\left({}^{\mathcal{N}}\hat{\boldsymbol{n}}^T [BN]^T {}^{\mathcal{B}}\hat{\boldsymbol{b}}\right)$
3: **if** $\theta < \theta_{0\min} = \frac{1}{2}\frac{I}{u_{\max}}\omega_{\max}^2 + \theta_{\min}$ **then**
4: Use constrained control given in Equation (39)
5: **else if** $\theta > \theta_{0\max} = \theta_{0\min} + \psi$ **then**
6: Use unconstrained control given in Equation (11)
7: **end if**

This algorithm is repeated for every single exclusion constraint. Therefore, at a given instant of time, some constraints will be considered while others will not. That means eliminating those constraints that are not considered in Equations (36) and (37).

$$-\ln\left(-\frac{C_i^E(\boldsymbol{\sigma}_{\mathcal{B}/\mathcal{N}})}{\alpha_i}\right) \to 1 \tag{49}$$

$$\frac{([{}^{\mathcal{B}}\tilde{\boldsymbol{b}}][BN]^{\mathcal{N}}\hat{\boldsymbol{n}})}{C_j^E(\boldsymbol{\sigma}_{\mathcal{B}/\mathcal{N}})} \to 0 \tag{50}$$

In order to reduce (but not eliminate) the discontinuity while switching, the parameter α_i in Equation (37) can be chosen as

$$\alpha_i = |\cos(\theta_{0\max}) - \cos(\theta_{\min})|e \tag{51}$$

such that the logarithm in Equation (49) switches continuously when turning off the constraint algorithm.

NUMERICAL RESULTS

The simulation shown utilizes the parameters indicated in Table 1. Four identical reaction wheels in a pyramid configuration with an angle of 55° are used. The initial attitude is a simple rotation of 135° about the $\boldsymbol{x}$ axis. The initial angular velocity is full speed ($\omega_{\text{max}} = 2^\circ/s$) in the same direction. The four reaction wheels are spinning at nominal speed (200 rpm). The control loops run at different frequencies: the servo has a frequency of 100 Hz; the steering law, 10 Hz. Four exclusion constraints are used with an optical payload in the $\boldsymbol{y}$-body direction. One inclusion constraint, with an antenna in the $\boldsymbol{x}$-body direction is also setup.

Table 1. Simulation parameters.

Spacecraft	$[I_S]$ $[kg\text{-}m^2]$	diag($[4.415 \quad 4.415 \quad 3.83]$)
RW	$[I_w]$ $[kg\text{-}m^2]$	diag($[0.03 \quad 0.001 \quad 0.001]$)
	$[G_s]$	$\begin{bmatrix} 0.819 & 0 & -0.819 & 0 \\ 0 & 0.819 & 0 & -0.819 \\ 0.5736 & 0.5736 & 0.5736 & 0.5736 \end{bmatrix}$
	$u_{s_{\text{max}}}$	$15mNm$
Initial Conditions	$\boldsymbol{\sigma}_{\mathcal{B}/\mathcal{N}_0}, \boldsymbol{\omega}_{\mathcal{B}/\mathcal{N}_0}$	$[-0.67 \quad 0 \quad 0]^T$, $[\omega_{\text{max}} \quad 0 \quad 0]^T$
	$[\Omega_1 \quad \Omega_2 \quad \Omega_3 \quad \Omega_4]_0^T$	$[200 \quad -200 \quad 200 \quad -200]^T$ rpm
Control Constants	$[P]$	$10[I_{3\times3}]$
	$[K_I]$	$0.01[I_{3\times3}]$
	K_1, K_3	0.1
Exclusion Constraints	${}^{\mathcal{N}}\hat{\boldsymbol{n}}_{\boldsymbol{1}}, {}^{\mathcal{B}}\hat{\boldsymbol{b}}_{\boldsymbol{1}}, \theta_{\text{min1}}$	$[0 \quad -0.34 \quad -0.96]^T$, $[0 \quad 1 \quad 0]^T$, 10°
	${}^{\mathcal{N}}\hat{\boldsymbol{n}}_{\boldsymbol{2}}, {}^{\mathcal{B}}\hat{\boldsymbol{b}}_{\boldsymbol{2}}, \theta_{\text{min2}}$	$[0 \quad -1 \quad 0]^T$, $[0 \quad 1 \quad 0]^T$, 30°
	${}^{\mathcal{N}}\hat{\boldsymbol{n}}_{\boldsymbol{3}}, {}^{\mathcal{B}}\hat{\boldsymbol{b}}_{\boldsymbol{3}}, \theta_{\text{min3}}$	$[1 \quad 1 \quad 0]^T$, $[0 \quad 1 \quad 0]^T$, 20°
	${}^{\mathcal{N}}\hat{\boldsymbol{n}}_{\boldsymbol{4}}, {}^{\mathcal{B}}\hat{\boldsymbol{b}}_{\boldsymbol{4}}, \theta_{\text{min4}}$	$[-1 \quad 1 \quad 0]^T$, $[0 \quad 1 \quad 0]^T$, 20°
Inclusion Constraints	${}^{\mathcal{N}}\hat{\boldsymbol{n}}_{\boldsymbol{5}}, {}^{\mathcal{B}}\hat{\boldsymbol{b}}_{\boldsymbol{5}}, \theta_{\text{min5}}$	$[1 \quad 0 \quad 0]^T$, $[1 \quad 0 \quad 0]^T$, 60°

Algorithm 1 is used for saddle-point avoidance with $\gamma = 0.05$. Algorithm 2 is used for switching between the constrained and unconstrained laws. In order to compute the threshold angle, u_{max} is chosen to be 40% of the minimum torque capacity computed with Equation (46). A gap of $\psi = 5^\circ$ is used.

Figure 4 shows the attitude state and the attitude difference. Figure 5 shows the evolution of the five angles angles θ_1, θ_2, θ_3, θ_4, and θ_5. The black dotted lines indicate the cone angles. The minimum and maximum threshold, in cyan and magenta respectively, are the switching angles described in Algorithm 2. The conical projections of the boresight vector of each instrument, along with the exclusion (in red) and inclusion (in green) zones is shown in Figure 6.

CONCLUSIONS

This paper has presented a kinematic steering law that can be used to control, in a regulation or tracking problem, the attitude of a spacecraft with reaction wheels under static constraints. The scheme is suitable for both inclusion and exclusion zones. It has been shown that the algorithm works with any number of constraints, even in highly-symmetric conditions. Moreover, it is possible, if desired, to switch from the constrained steering law to the unconstrained steering law when sufficiently far from the constraint cones.

One of the main advantages of using Lyapunov theory is to be able to synthesize control laws that, though nonlinear, are fairly simple. The algorithm described in this paper allows controlling the attitude of a spacecraft under constraints using MRPs while separating the dynamics from the kinematics.

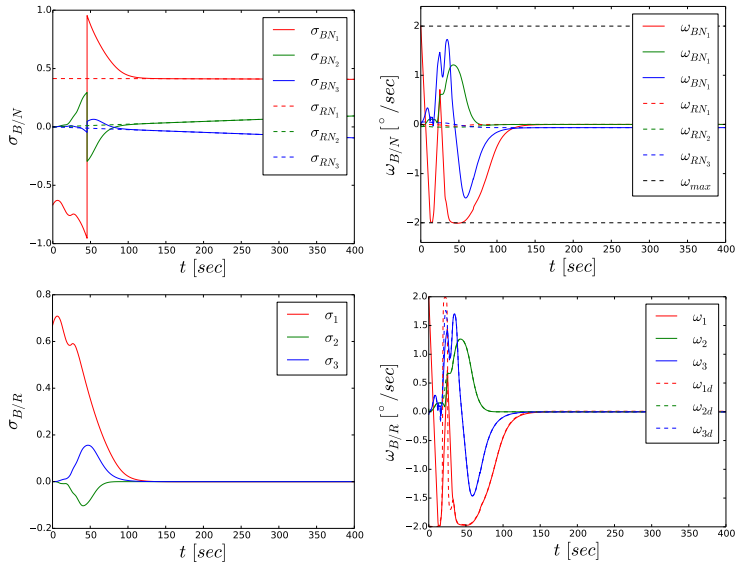

Figure 4. Attitude state evolution in the tracking problem.

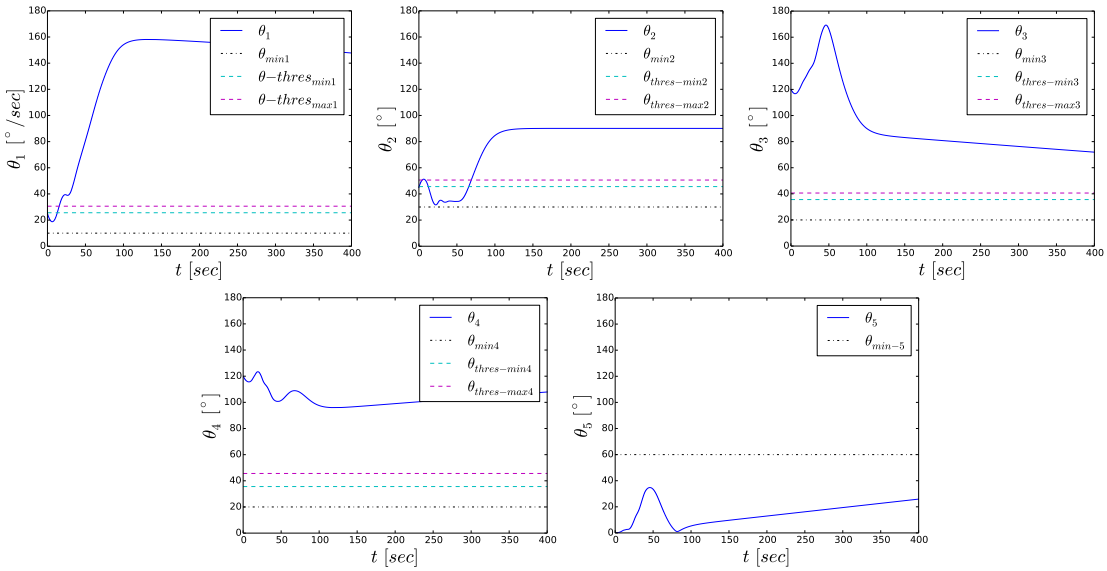

Figure 5. Constraint angles.

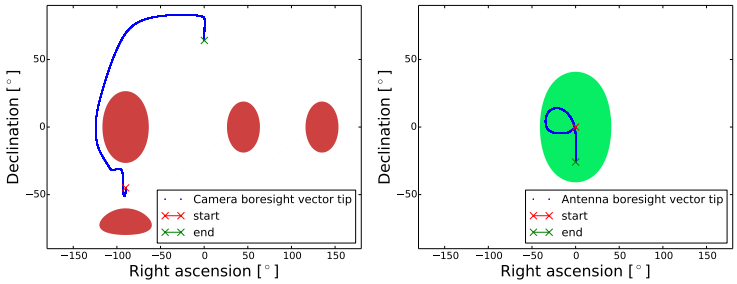

Figure 6. 2-D maps in the tracking problem.

There are several questions that can be addressed in future work. First, the algorithm for escaping from saddle points has been explained heuristically, but not mathematically. Second, the algorithm switching between constrained and unconstrained laws still present some discontinuities. Future work could address further smoothing techniques for switching between both. Third, it is still to be seen whether the control scheme can be extended to develop Lyapunov functions that simultaneously include attitude and angular velocity.

REFERENCES

[1] Y. Kim, M. Mesbahi, G. Singh, and F. Hadaegh, "On the Convex Parameterization of Spacecraft Orientation in Presence of Constraints and its Applications," *IEEE Transactions on Aerospace and Electronic Systems*, Vol. 46, No. 3, 2010, pp. 1097–1109.

[2] H. Hablani, "Attitude Commands Avoiding Bright Objects and Maintaining Communication with Ground Station," *AIAA Journal of Guidance, Control, and Dynamics*, Vol. 22, No. 6, 1999, pp. 759–767.

[3] K. Spindler, "New Methods in On-board Attitude Control," *Advanced in the Astronautical Sciences*, Vol. 100, No. 2, 1998, pp. 111–124.

[4] G. Singh, G. Macala, E. Wong, and R. Rasmussen, "A constraint monitor algorithm for the Cassini spacecraft," *Proceedings of the AIAA Guidance, Navigation, and Control Conference*, 1997, pp. 272–282.

[5] A. Ahmed, J. Alexander, D. Boussalis, W. Breckenridge, G. Macala, M. Mesbahi, M. San Martin, G. Singh, and E. Wong, *Cassini Control Analysis Book*. Jet Propulsion Laboratory, 1998.

[6] E. Frazzoli, M. Dahleh, E. Feron, and R. Kornfeld, "A Randomized Attitude Slew Planning Algorithm for Autonomous Spacecraft," *Proceedings of the AIAA Guidance, Navigation, and Control Conference*, 2001.

[7] Y. Kim and M. Mesbahi, "Quadratically Constrained Spacecraft Attitude Constrained Control Via Semidefinite Programming," *IEEE Transactions on Automatic Control*, Vol. 49, No. 5, 2004, pp. 731–735.

[8] C. Sun and R. Dai, "Spacecraft Attitude Control under Constrained Zones via Quadratically Constrained Quadratic Programming," *AIAA Guidance, Navigation, and Control Conference, AIAA SciTech*, 2015.

[9] H. Kjellberg and G. Lightsey, "Discretized Constrained Attitude Pathfinding and Control for Satellites," *AIAA Journal of Guidance, Control, and Dynamics*, Vol. 36, No. 5, 2013, pp. 1301–1309.

[10] S. Tanygin, "Fast Three-Axis Constrained Attitude Pathfinding and Visualization Using Minimum Distortion Parameterizations," *AIAA Journal of Guidance, Control, and Dynamics*, Vol. 38, No. 12, 2015, pp. 2324–2336.

[11] C. R. McInnes, "Large Angle Slew Maneuvers with Autonomous Sun Vector Avoidance," *AIAA Journal of Guidance, Control, and Dynamics*, Vol. 17, No. 4, 1994, pp. 875–877.

[12] U. Lee and M. Mesbahi, "Spacecraft Reorientation in Presence of Attitude Constraints via Logarithmic Barrier Potentials," *Proceedings of the American Control Conference*, 2011, pp. 450–455.

[13] U. Lee and M. Mesbahi, "Feedback Control for Spacecraft Reorientation under Attitude Constraints via Convex Potentials," *IEEE Transcactions on Aerospace and Electronic Systems*, Vol. 50, No. 4, 2014, pp. 2578–2592.

[14] U. Lee, *State-Constrained Rotational and Translational Motion Control With Applications to Monolithic and Distributed Spacecraft*. PhD dissertation, University of Washingtom, 2014.

[15] H. Schaub and J. L. Junkins, *Analytical Mechanics of Space Systems*. Reston, VA: AIAA Education Series, 3rd ed., 2014, 10.2514/4.102400.

[16] S. W. Sheppard, "Quaternion From Rotation Matrix," *AIAA Journal of Guidance and Control*, Vol. 1, No. 3, 1978, pp. 223–224.

[17] H. Schaub and S. Piggott, "Speed-Constrained Three-Axes Attitude Control Using Kinematic Steering," *AAS Guidance, Navigation and Control Conference*, 2017.

[18] H. Khalil, *Nonlinear Systems*. Prentice Hall, 3rd ed., 2002.

[19] K.-S. Kim and Y. Kim, "Robust Backstepping Control for Slew Maneuver Using Nonlinear Tracking Control," *IEEE Transactions on Control Systems Technology*, Vol. 11, No. 6, 2003, pp. 822–829.

[20] K. Tee, S. Ge, and E. Tay, "Barrier Lyapunov Functions for the Control of Output-Constrained Nonlinear Systems," *Automatica.*, No. 45, 2009, pp. 918–927.

[21] F. Landis Markley, R. Reynolds, F. Liu, and K. Lebsock, "Maximum Torque and Momentum Envelopes for Reaction-Wheel Arrays," *Journal of Guidance, Control, and Dynamics*, Vol. 33, No. 5, 2010, pp. 1606–1614.